Structural Eng. / Earthquake Eng. Vol. 3. No. 2, 417s-427s. October 1986
Japan Society of Civil Engineers (Proc. of JSCE No. 374 / I-6)

SEISMIC BEHAVIOR OF A ROCK TUNNEL

By Yasuki YAMAGUCHI, Mitsuru TSUJITA** and Kazushi WAKITA***

In order to investigate seismic behavior of a rock tunnel, earthquake observations have been carried out in the Shin Usami Tunnel of JNR's Line, located in Ito City of Shizuoka prefecture. From an analysis of earthquake records observed from July 1983 to June 1985, the following results were obtained.

① The direction of the predominant motion of an earthquake in rock which lies sufficiently deep below the surface is not necessarily closely related to the direction of the epicenter.

② As for the propagation of an earthquake, the primary wave of the initial motion and the shear wave of the main motion propagate in the upward direction nearly vertically.

③ The frequencies at the peaks of the amplification function are constant and not influenced by the properties of the earthquake. In the horizontal plane of the rock around a tunnel, no noticeable amplification of the earthquake wave can be seen even in the vicinity of a cavern.

④ In the cross section of a tunnel, the shearing deformation is significant.

Keywords: earthquake observation, rock tunnel, principal axis, wave propagation

1. INTRODUCTION

There have been number of constructions in rock caverns in Japan, including underground power plants, rock tunnels, etc. We may say some of these experienced large earthquakes. However, a quantitative method of evaluating seismic stability based on the observed data is yet to be established, and from the viewpoint that seismic designs providing high reliability will be required in the future utilization of rock caverns, it is considered necessary to understand the phenomena based on the observed data.

As the primary studies based on the observed data, study of Hayashi and Komada[1], study of Ichikawa[2], study of Hamada[3], and study of Tamura[4] can be mentioned. Also, on the earthquake disasters of tunnels, data have been reported by Dowding[5], and by Yoshikawa[6].

However, the propagation of earthquake motion in the rock surrounding a cavern, and accompanying deforming behavior of the cavern are still to be clarified further, judging from the fact that studies of this type are still short in their history and there are but a few observations. Therefore, it is considered necessary to accumulate observed data, and continuously conduct detailed analyses based on these data.

Therefore, in order to clarify the seismic behavior of a cavern and surrounding rock based on the observed data, we, in cooperation with JNR, carried out earthquake observations in Shin-Usami Tunnel of JNR's Itoh Line started July, 1983, and conducted a study on the seismic behavior of a cavern and surrounding rock based on these observed data[9)~11)]. After 2 years of observation, 50 earthquakes including the earthquake swarm (35 earthquakes occured in the eastern offshore of Izu Peninsula in September,

* Member of JSCE, Eng. Manager, Technical Research Institute, Hazama-Gumi, Ltd.
** Members of JSCE, M. Eng., Technical Research Institute, Hazama-Gumi, Ltd.
(17-23, Nishi 4-chome Honmachi, Yono City, Saitama Prefecture 338, Japan)

1984) have been observed.

This report deals with the propagation of earthquake motion in deep rock at 260 m from the surface, and accompanying deforming behavior of a cavern, based on the waveform analyses of the observation records obtained during the period between July, 1983 through June, 1985.

2. OUTLINE OF OBSERVATION AND OBSERVATION RECORDS

Shin-Usami Tunnel, of Itoh Line, is a single tracked railway tunnel having a 3 000 m of overall length to be constructed in Itoh City, Shizuoka Pref. Its internal cross section has a circular form with inner diameter of 6 m, and the lining concrete is 30 cm in thickness. The observation section is a 100 m section located at approx. 1 500 m from each entrance, and the depth from top of the mountain is approx. 260 m. The observation section is composed mainly of Alternated Basalt, and the velocity of the S wave V_s is 1.1 to 1.6 km/sec. Fig. 1 shows the outline of the tunnel and the observation section.

The earthquake observation is carried out at Usami Entrance and in the observation section, using 8 accelerometers including one at the Entrance, 10 strain gauges set on the lining concrete, and 6 strain gauges set in the rock. Fig. 2 and Fig. 3 show the layout of measuring instruments for the earthquake observation. Additionally, each of 8 acceleromaters has the three components of X, Y and Z : the X-direction is the direction of tunnel axis (N 13°23′35″E), Y-direction is normal to the tunnel axis (S 76°36′25″E), and Z-direction is vertical to the tunnel axis. The accelerometers used are the servo type (SA-355) with measurable range of frequency 0.1 to 30 Hz and the minimum resolution 0.01 gal. The strain gauges are the differential trans type (SD-100) for the lining concrete portion and (DIS-300) for the rock portion, both having the measurable range of frequency 0.1 to 30 Hz and the minimum resolution 0.03×10^{-6}. Earthquake waves are recorded by digital earthquake wave recorder (SAMTAC-120 D-64). The input filter of the recorder is DC-30 Hz, and the sampling time is 10 msec (100 Hz). The measuring unit is set so as to be triggered when anyone of the 3 components of the A-6 accelerometer installed 40 m below the tunnel's bottom receives 0.3 gal. Additionally, recording is started 3 sec before the triggered time by means of the delay unit.

Fig. 4 shows the position of epicenters of the earthquakes observed, and Table 1 shows a list of the observation records. As the examples of the observation records, the X, Y and Z components of the acceleration waveform in rock measured by accelerometer A-4 at No. 3 and No. 5 earthquakes are shown in Fig. 5 and Fig. 6. Also, the power spectrums of the acceleration, velocity and displacement at A-4, of the same earthquakes, are shown in Fig. 7 and Fig. 8.

3. PRINCIPAL AXIS OF EARTHQUAKE

(1) Calculation method for principal axis of earthquake

To clarify the properties of earthquake motion in rock approx. 260 m from the surface, firstly the principal axes of observed earthquakes were studied.

When an earthquake motion presenting a three-dimensional movement is separated into 3 vibrational

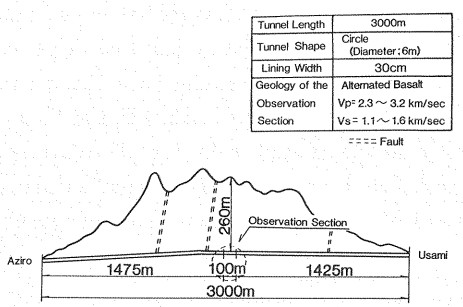

Fig. 1 Outline of Tunnel and Observation Section.

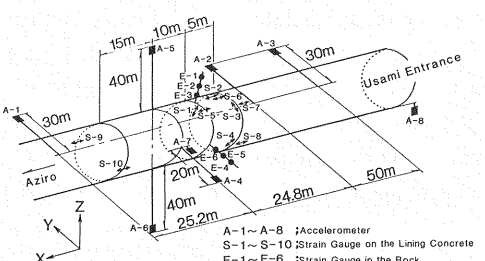

Fig. 2 Layout of Measuring Instruments.

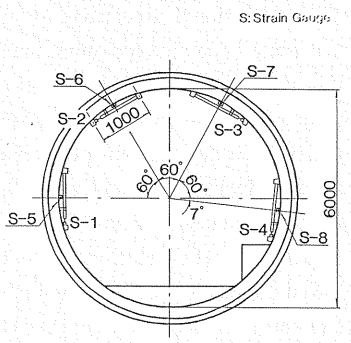

Fig. 3 Layout of Strain Gauges on the Lining Concrete (View from Aziro).

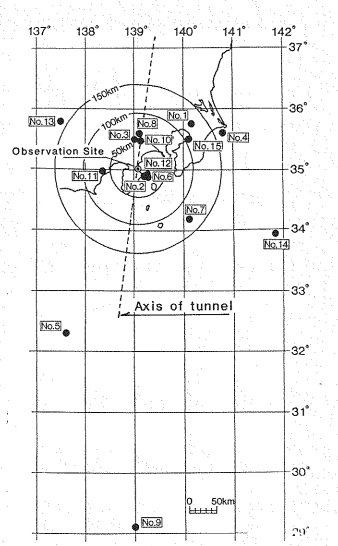

Fig. 4 Epicenters of Observed Earthquakes.

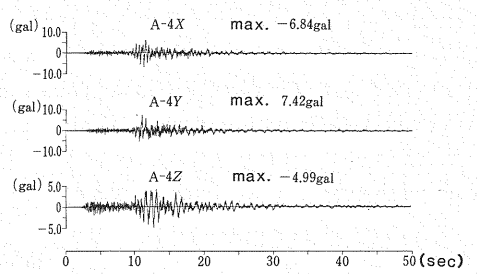

Fig. 5 Acceleration Waveform in Rock (Earthquake No. 3).

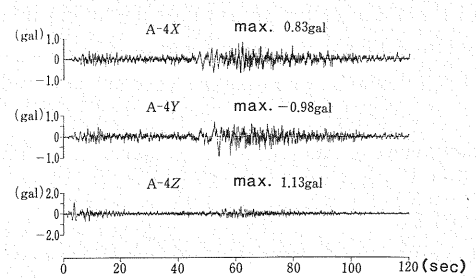

Fig. 6 Acceleration Waveform in Rock (Earthquake No. 5).

Table 1 Maximum Values of Observation Record.

No.	Data	M	H (km)	D (km)	Observed Data A (gal) R	A (gal) E	S (μ) C	S (μ) L
1	1983.7.13	4.2	123.1	73	0.49	1.53	0.07	0.03
2	1983.7.27	2.9	18.8	15	1.33	0.78	0.20	0.04
3	1983.8.8	6.0	51.7	22	7.42	15.21	8.84	1.77
4	1983.12.30	5.4	166.9	60	0.60	2.28	0.41	0.10
5	1984.1.1	7.5	328.1	340	1.12	2.09	2.22	0.65
6	1984.1.12	3.3	25.0	10	1.42	2.49	0.35	0.06
7	1984.2.13	5.3	130.0	90	0.64	1.89	0.30	0.13
8	1984.2.14	5.3	62.5	20	0.99	2.77	0.87	0.16
9	1984.3.6	7.9	656.3	400	2.57	2.94	3.10	1.61
10	1984.6.26	4.6	50.5	20	2.39	3.29	0.62	0.09
11	1984.8.13	4.8	66.4	21	1.55	4.76	0.44	0.06
12–1 ~ 35	1984.9.1 ~ 9.26	3.0 ~ 4.7	3.3 ~ 23.0	0 ~ 21	15.03		2.86	0.50
13–1	1984.9.14	6.9	163.6	0	1.89	8.29	1.97	0.54
13–2	1984.9.15	6.2	167.8	0	1.71	4.29	1.80	0.33
14	1984.9.19	6.8	278.6	46	2.01	5.31	2.25	0.37
15	1985.1.7	5.1	106.6	70	2.42	6.25	0.39	0.34

M: Magnitude
H: Epicentral distance
D: Epicentral depth
A: Maximum horizontal acceleration
S: Maximum strain
R: in the rock
E: at the entrance
C: lining circumeferential
L: lining Axial

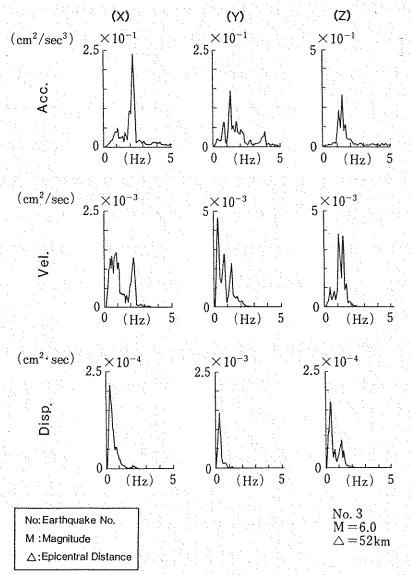

Fig. 7 Power Spectrum of the No. 3 Earthquake (A-4).

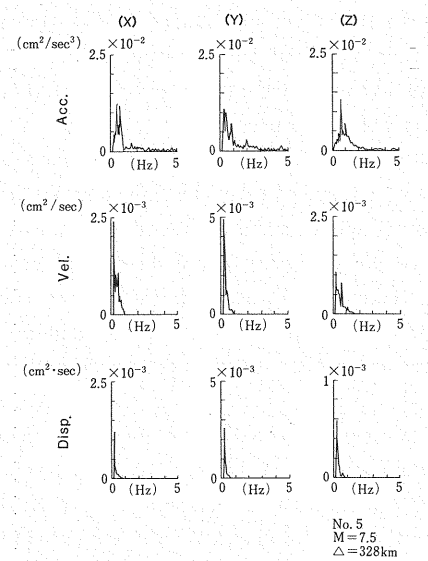

Fig. 8 Power Spectrum of the No. 5 Earthquake (A-4).

directions any 2 of which are at right angles to each other, these 3 vibrational directions are called the principal axes of earthquake motion along which the vibrational energy becomes maximum, medium and minimum, respectively.

By studying the above-mentioned 3 directions and the distribution of the observed values around these directions using the special distribution of the acceleration, velocity and displacement of the earthquake motion obtained by observation instruments having 3 directional components (vertical and 2 horizontal components), the properties of observed earthquake motion can be clarified three-dimensionally.

In other words, by clarifying the direction of maximum principal axis, the relationship between the vibrational direction along which the vibrational energy of earthquake motion becomes dominant and the directions of the 3 components (vertical and 2 horizontal components) of observed earthquake motion becomes clear. Also, by clarifying the dispersion of the observed values around the maximum principal axis from the distribution of observed values, a degree that the 3 components (vertical and 2 horizontal components) of observed earthquake motion are governed by the vibration in the direction of maximum principal axis becomes clear.

Here, 5 earthquakes ; No. 3, No. 5, No. 9, No. 13-1, and No. 14 are selected, and the principal axes of earthquake motion in rock and the dispersion of observed values around the principal axes are studied. In calculating the principal axes of earthquake motion ; ① principal axis Ⅰ ··· the principal axes varying in time domain (t), where the cross power spectrum at the time (t) becomes the maximum, medium and minimum, and ② principal axes Ⅱ ··· the fixed principal axes, along which the total energy becomes the maximum, medium and minimum are used out of the methods using the cross power spectrum proposed by Hoshiya[7]. Additionally, the total energy is the power spectrum along the principal axes integrated in frequency domain and time domain.

(2) Direction of fixed principal axes

Conventionally, the following reports have been made on the direction of the fixed principal axes of earthquake motion by Watabe[8], Hoshiya[7] and Hamada[3] :

① The fixed maximum principal axis along which the total energy of earthquake motion is the largest presents favorable correspondence with the direction connecting the observation point and epicenter[8].

② The intermediate axis which extends normal to the fixed maximum principal axis presents favorable correspondence with the direction connecting the observation point and epicenter[3),7)].

③ The fixed maximum principal axis is nearly horizontal[7),8)].

These items are considered to be significant in that, in setting the input earthquake motion of a structure, its dominant vibrational direction can be set corresponding to the direction of the point where earthquakes are generated, and that its incident direction can be restricted to a near vertical direction around the structure.

However, as it is understood from above ① and ②, the correspondence of the fixed axes and epicenter has not yet specifically described at the moment.

Also, reports made by Watabe[8] and Hoshiya[7] are based on the earthquake motion observed in near surface. In designing any underground structure, it is necessary to study the fixed axes of observed earthquakes deep in rock, however, regarding this point, there are only a few studies including that of Hamada and his group made on the incident direction of earthquake motion using fixed axes[3]. And these studies are mostly based on acceleration records, and naturally velocity and displacement are not studied there.

In this report, the direction of fixed principal axes in deep rock is studied using acceleration, velocity and displacement records.

Table 2 shows the horizontal and vertical angles of fixed axes of earthquake motion in rock (A-4). Here, the horizontal angle is the one extending from the X-axis to the Y-axis at the observation point and the vertical angle is the one extending from the Z-axis to the $X-Y$ plane. Here, we discuss the results at

A-4, the same tendency can be obtained at any other point in Rcok.

Fig. 9 shows the direction in horizontal plane ($X-Y$ plane) and the direction in vertical plane ($Z-X$, Y plane) of the fixed principal axes of earthquake motion in rock A-4. From Fig. 9, the following can be mentioned on the direction of the fixed principal axes in rock :

① In the earthquake No. 3, the fixed intermediate principal axis of velocity and displacement show favorable correspondence to the direction of epicenter. For acceleration, both the maximum and intermediate principal axes cannot be said to be favorable in terms of their correspondence to the epicenter.

② In the earthquake No. 5, the intermediate principal axis is near the direction of epicenter for acceleration, velocity and displacement, and the correspondence is particularly favorable about displacement followed by velocity and acceleration in this order.

③ In the earthquake No. 9, for acceleration, velocity and displacement, the fixed maximum principal axis is relatively near the epicenter, but the degree of correspondence cannot be said to be favorable.

④ In the earthquake No. 13-1, the fixed intermediate principal axis of acceleration presents a favorable correspondence to the epicenter. For velocity and displacement, the fixed maximum principal axis is relatively near the direction of epicenter, however, the correspondence cannot be said to be favorable.

⑤ In the earthquake No. 14, for acceleration, velocity and displacement, the fixed maximum principal axis is near the direction of epicenter, and the correspondence is relatively favorable for displacement, followed by velocity and acceleration.

⑥ In each earthquake, the maximum principal axis is near the horizontal plane.

Conventionally, there have been reports on the direction of the fixed principal axes in horizontal plane of earthquake motion as aforementioned, one insisting that the maximum principal axis and the direction of epicenter show a favorable correspondence[8], and ones insisting that the intermediate principal axis and the direction of epicenter show a favorable correspondence[3),7)]. According to this study performed in a deep

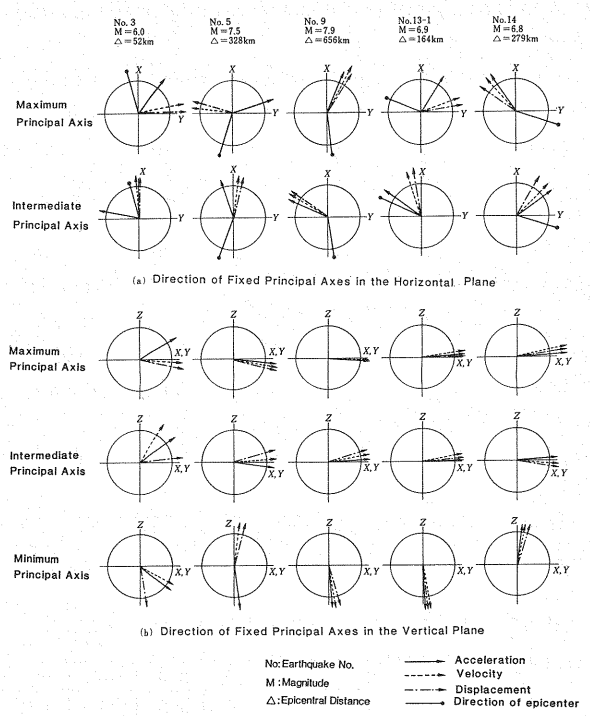

Fig. 9 Direction of Fixed Principal Axes in Rock (A-4).

Table 2 Horizontal and Vertical angles of Fixed axes of Earthquake Motion in Rock (A-4).

	No	Maximum Principal Axis		Intermediate Principal Axis		Minimum Principal Axis	
		θ_H	θ_V	θ_H	θ_V	θ_H	θ_V
Acc.	3	37.8	59.0	-79.5	52.6	-25.0	127.2
	5	71.8	96.0	-18.8	96.3	154.7	171.3
	9	25.4	91.4	-64.5	85.4	-81.9	175.2
	13-1	33.7	84.2	-56.4	89.0	23.7	174.1
	14	-36.0	82.9	54.3	87.7	162.4	7.5
Vel.	3	80.4	93.7	-3.7	32.3	-11.9	122.0
	5	-82.1	97.6	7.6	87.5	-100.6	8.0
	9	28.2	92.8	-61.3	79.4	-76.2	169.1
	13-1	72.0	84.7	-18.6	82.8	17.7	171.0
	14	-42.0	77.4	47.5	92.0	128.8	12.8
Disp	3	88.6	99.8	-0.1	82.5	-53.3	167.7
	5	-75.6	99.2	12.0	75.7	-133.9	17.1
	9	30.0	90.8	-59.8	74.5	-62.8	164.4
	13-1	77.7	86.5	-12.6	84.9	21.7	173.8
	14	-55.5	77.1	33.1	95.8	99.5	14.2

No : Earthquake No
θ_H : Horizontal angles (deg)
θ_V : Vertical angles (deg)

rock, however, both the maximum and intermediate principal axes can be considered to have the possibility to become relatively near the direction of epicenter, and it is rather difficult to define the nearest of the two.

Also, the degree of correspondence of these principal axes with the direction of epicenter cannnot be said to be so good as was said conventionally, as a whole. As the reason for this, it may be pointed out that the dominant vibration direction in earthquake motion is influenced not only by the direction of epicenter, but also by the geology along a path through which the earthquake motion propagates to reach the observation point, topographical variation, or reflection and refraction of wave motion at the observation point.

As for the direction of fixed maximum principal axis in a vertical plane, it is considered to be near the horizontal direction, as was reported conventionally[7),8)]. Consequently, it can be assumed that, near the observation point, the earthquake motion propagates vertically in any earthquakes.

(3) Distribution of observed values around the fixed maximum principal axis

The degree of dispersion of observed values around the fixed maximum principal axis is studied using the ratio of total vibrational energy λ_2 in the direction of intermediate principal axis and that λ_3 in the direction of minimum principal axis to the total vibrational energy λ_1 in the direction of maximum principal axis, namely λ_2/λ_1 and λ_3/λ_1.

The degree of dispersion of observed values around the maximum principal axis can be assumed by the size of λ_2/λ_1 and λ_3/λ_1. The dispersion is considered large when λ_2/λ_1 or λ_3/λ_1 is closed to 1 (one), or it is considered small when both of these ratios is near 0 (zero).

Table 3 shows the λ_2/λ_1 and λ_3/λ_1 obtained from acceleration, velocity and displacement in rock A-4.

From the values shown in the table, the following can be assumed:

① For acceleration, both λ_2/λ_1 and λ_3/λ_1 are large. From this fact, it is assumed that the observed values show a large three-dimensional dispersion around the maximum principal axis.

② For velocity and displacement, λ_2/λ_1 is large, but λ_3/λ_1 tends to become smaller than λ_2/λ_1. Therefore, for velocity and displacement, it is assumed that a large two-dimensional dispersion exists in the plane formed with fixed maximum and intermediate principal axes.

From above findings, it is considered that, in rock, there is a large dispersion around the maximum principal axis. Therefore the degree that the three directional components of observation (vertical and 2 horizontal components) are affected by the predominant vibrational direction of earthquake motion, is considered small.

(4) Maximum principal axis varying in time domain (t)

In order to clarify the variation of the direction of the predominant vibration during the duration time of an earthquake motion, here, putting eyes on the maximum principal axis of the acceleration in rock, the degree of its variation in time domain is studied.

In studying the variation in time domain, principal axes varying in the time domain (t) (axes varying in the time domain (t) where the cross power spectrum at the time (t) becomes the maximum, medium and minimum) are used. Additionally, the variation of the principal axes in time domain is calculated with 1 sec intervals. Also, the range of integration in time domain of the cross power spectrum used for obtaining the principal axes varying in time domain (t) is set to be 5 sec around the time (t).

Table 3 Ratio of Total Vibrational Energy in the Direction of Fixed Principal Axis.

No	Acc.		Vel.		Disp.	
	λ_2/λ_1	λ_3/λ_1	λ_2/λ_1	λ_3/λ_1	λ_2/λ_1	λ_3/λ_1
3	0.76	0.63	0.70	0.45	0.26	0.17
5	0.93	0.86	0.61	0.40	0.43	0.23
9	0.43	0.24	0.40	0.20	0.55	0.26
13-1	0.65	0.31	0.62	0.21	0.33	0.09
14	0.90	0.60	0.68	0.35	0.40	0.16

No : Earthquake No

Fig. 10 shows the variation in time domain of the horizontal and vertical angles of the maximum principal axis of acceleration in rock A-4 for each earthquake.

From Fig. 10, the following are clarified on the variation

in time domain of the maximum principal axis :

① The variation in time domain of the maximum principal axis is large for both horizontal and vertical angles.

② For earthquakes No. 3 and No. 5 in which both initial and main earthquake motions are obtained judging from the observed waveform, the vertical angle of the maximum principal axis is near 0° or 180° during the initial motion, and it varies largely around 90° during and after the main motion.

From above findings, the principal axes of earthquake motion cannot be said to be fixed throughout the duration time of an earthquake motion, and particularly during and after the main motion, they are considered to vary largely. As the reason for such a large variation of the principal axes, it may be pointed out that the vibrational direction of earthquake motion tends to be influenced by the geology along a path through which the earthquake motion propagates to reach the observation point, topographical variation, or reflection and refraction of wave motion at the observation point.

Also, the fact that the vertical angle of maximum principal axis is near 0° or 180° during the initial motion and it varies around 90° during and after the main motion, is presumably indicating that, during the initial motion, the primary wave becomes eminent, making the vertical motion predominant, and during and after the main motion, the shear wave becomes eminent, making the horizontal motion predominant.

Thus an earthquake motion changes from the initial motion where the primary wave becomes predominant to the main motion where the shear wave becomes predominant, indicating complicated three-dimensional characteristics. Therefore, the principal axes vary and it is considered difficult to fix the principal axes during the duration time.

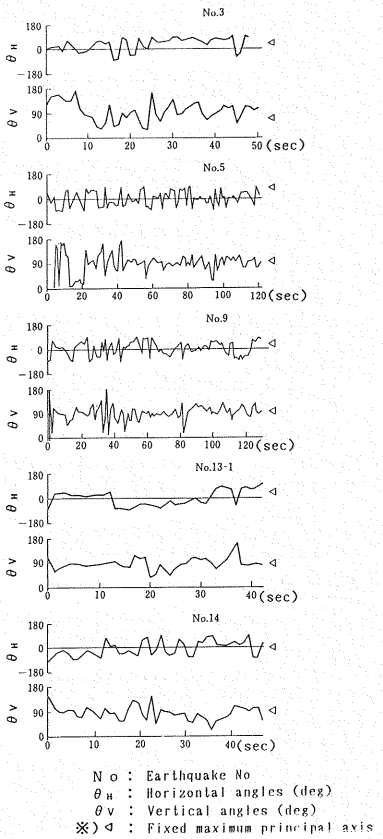

Fig. 10 Variation of Maximum Principal Axis in Time Domain (A-4).

(5) Variation of the maximum principal axes at each point in rock

Fig. 11 shows the variations in time domain of the horizontal and vertical angles of maximum principal axis at each of the points A-1 through A-7 in rock around a cavern during the earthquake No. 3, for acceleration, velocity and displacment.

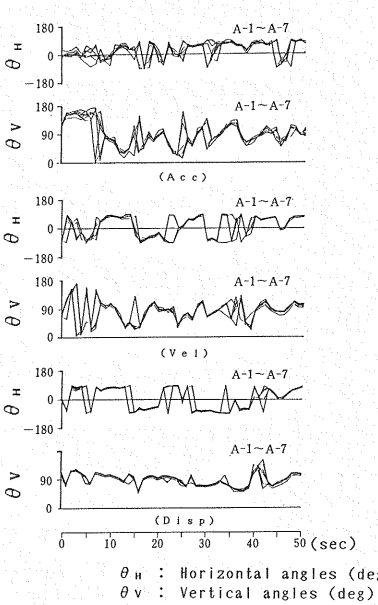

Fig. 11 Variation of Maximum Principal Axis in Time Domain (A-1~A-7), No. 3 Earthquake.

From Fig. 11, it is understood that the variation in time domain of the maximum principal axis at each point in rock around the cavern is nearly equal to each other. Consequently, it is considered that the points in rock around the cavern of the observation section vibrate three-dimensionally almost together and, therefore, the phase difference of earthquake motions between each two points are small.

From above finding, every point in a volume of rock ranging from 60 to 100 cubic meters formed by points A-1 through A-7 around the cavern, when viewed from the absolute system of coordinates, can be considered to present a uniform but relatively complicated three-dimensional behavior.

Additionally, this tendency can be also seen in the earthquakes No. 5, 9, 13-1 and 14.

4. WAVE PROPAGATION OF EARTHQUAKE MOTION

In the foregoing chapter, the three-dimensional characteristics of an earthquake and the properties of wave propagation were clarified. In this chapter, the properties of wave propagation is analysed from the spectrum ratio and the cross-correlation coefficient. Additionally, the data observed from 4 earthquakes No. 3, 4, 5 and 9 are used for the analysis.

The spectrum ratio of the acceleration waveform of the observation point A-5 at 40 m vertically above the tunnel to that A-6 at 40 m vertically below the tunnel is shown in Fig. 12, and the same of the observation point A-7 at 1 m horizontally aside the tunnel to that A-4 at 20 m horizontally aside the tunnel is shown in Fig. 13. Also, the spectrum ratio of shear wave obtained by using the one-dimensional wave propagation theory (SHAKE) and its analysis model is shown in Fig. 14.

From Fig. 12, it is assumed that, regarding the propagation of vertical earthquake motion, the

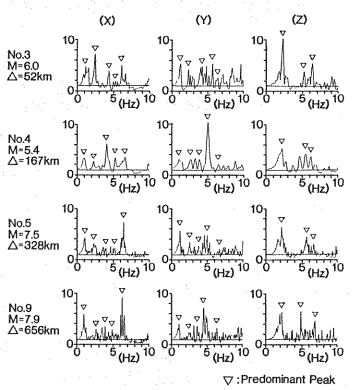

Fig. 12 Spectrum Ratio of Acceleration (A-5/A-6).

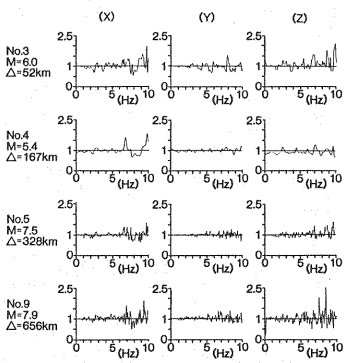

Fig. 13 Spectrum Ratio of Acceleration (A-7/A-4).

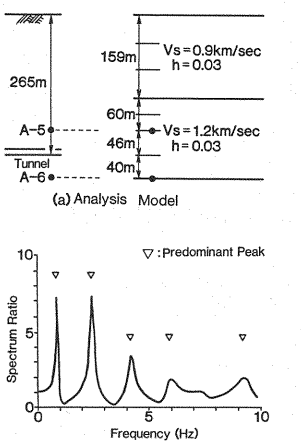

Fig. 14 Spectrum Ratio Obtained from One-Dimensional Wave Propagation Theory.

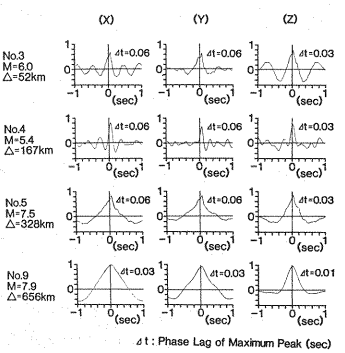

Fig. 15 Cross-Correlation Coefficient (A-5 and A-6).

frequency of the predominant peak of spectrum ratio is nearly constant for any earthquake, for both horizontal and vertical vibrations. Also, from Fig. 12 and Fig. 14, particularly the frequency of the predominant peak of spectrum ratio of horizontal vibration shows a favorable correspondence with that obtained by the one-dimensional wave propagation theory.

Judging from Fig. 13, however, it can be pointed out that there is not any eminent trend of amplification between horizontal two points near the tunnel for both horizontal and vertical vibrations within the range of 6 Hz and below where the frequency component of earthquake motion is presumably dominant.

Fig. 15 and Fig. 16 show the cross-correlation coefficients, about accerelation waveform, between A-5 and A-6, and A-4 and A-7, respectively. When the propagation velocity is constant and independent of frequency, the propagation velocity can be estimated as $V=L/\Delta t$, where L is the distance between 2 points along the direction of wave propagation and Δt is the phase lag. Both A-5 and A-6 are considered to be located along the direction of wave propagation. Table 4 shows the propagation velocity of waveform between A-5 and A-6 obtained from Fig. 15. Except for the earthquake No. 9, the propagation velocity in the vertical direction of the horizontal vibration and vertical vibration, as shown in Table 4, shows a favorable correspondence to the shear wave velocity and the primary wave veloctity obtained from the velocity logging.

For the earthquake No. 9, it is considered from the cross-correlation coefficients shown in Fig. 15 that the low-frequency component is particularly eminent. Therefore, it is assumed that the propagation velocity of No. 9 earthquake is larger than that of other earthquakes due to the influence of dispersing characteristic of the wave motion. Additionally, when this is taken as the propagation velocity of the surface wave, the propagation velocty is required to be obtained between the observation points along the surface. So, it is difficult to identify the propagation velocity of the earthquake No. 9 at the present situation.

From Fig. 16, it is seen that, about 2 points in the horizontal direction, the phase lag is nearly zero. From this, it can be assumed that the motion is nearly identical between 2 points near the tunnel and apart in the horizontal direction.

5. WAVE PROPAGATION AND THE DEFORMATION MODE OF A CAVERN

In the case of this observation site, V_s is 1 to 2 km/sec, and from the observed results, the predominant period of the spectrum of earthquake motion is 1 to 2 sec for earthquakes in remote places and 0.3 to 0.5 sec for those in near places. Therefore, the wavelength passing the cavern is estimated as 1 000 to 4 000 m at the longest, and 300 to 1 000 m at the shortest. Since the tunnel currently observed has a circular cross section of 6 m in inner diameter, the ratio of the diameter of the tunnel to wavelength of incident wave is 1/170 to 1/670 for long wavelengths and 1/50 to 1/170 for short wavelengths, and it is considered that a first shearing mode is dominant in the cavern in each case.

In order to study this in conjunction with the strain wave in the circumferential direction of the cavern,

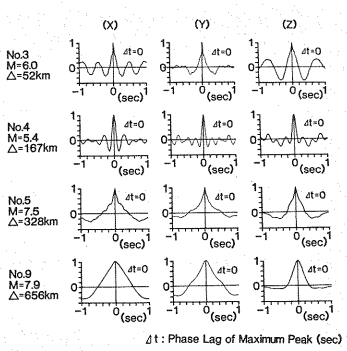

Fig. 16 Cross-Correlation Coefficient (A-4 and A-7).

Table 4 Propagation Wave Velocity Obtained from Cross-Correlation (A-5 and A-6).

No.	Propagation Wave Velocity (km/sec)		
	X	Y	Z
3	1.43	1.43	2.87
4	1.43	1.43	2.87
5	1.43	1.43	2.87
9	2.87	2.87	8.6
Result of Velocity Logging	Vs=1.1 ~ 1.6		Vp=2.3 ~ 3.2

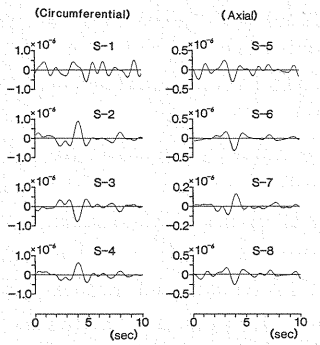

Fig. 17 Filtered Strain of the Lining (Earthquake No. 5).

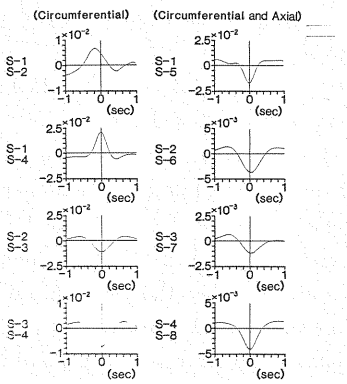

Fig. 18 Cross-Correlation of Strain of the Lining (Earthquake No. 5).

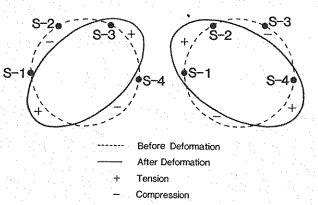

Fig. 19 Deformation Mode of the Cross Section of a cavern.

the phase of waveform of the observed wave applied with narrow-band pass filter for frequencies near the dominant frequency is analysed.

Fig. 17 relates to the earthquake No. 5 and shows the strain waveforms S-1, S-2, S-3 and S-4 in the circumferential direction of tunnel lining during the main motion for 10 sec, and those in the axial direction (S-5, S-6, S-7 and S-8) of the same. In order to distinguish the correlation of waveforms, these waveforms are applied with 0.2-1.2 Hz narrow-band pass filter where the power spectrum of strain is eminent.

From Fig. 17, by comparing the time history of the main motions among S-1, S-2, S-3 and S-4, the phase of S-1, S-2 and S-4 is nearly the same, and that of S-3 is reverse of those. Also, by comparing the circumferential strains S-1, S-2, S-3 and S-4 with the axial strains S-5, S-6, S-7 and S-8, the phases of the latters (S-5, S-6, S-7 and S-8) are nearly reverse of the formers (S-1, S-2, S-3 and S-4), respectively. From this, it is assumed that circumferential strains are coupled with the axial strains. Additionally, this trend is also seen in earthquakes No. 3, No. 4 and No. 9.

Fig. 18 relates to the earthquake No. 5 and shows the cross-correlations of strains in tunnel lining, where, the cross-correlations of circumferential strains, and that of circumferential strains and corresponding axial strains are shown.

From Fig. 18, the values of the cross-correlation of circumferential strains show the positive max. in the cross-correlations of S-1 and S-2, and S-1 and S-4, and the negative max. in the cross-correlations of S-2 and S-3, and S-3 and S-4. For the cross-correlation between the circumferential strains and axial strains, the values tend to show the negative max. in each case. Additionally, this trend is similarly seen in earthquakes No. 3, No. 4 and No. 9.

From the waveform of circumferential strains and the cross-correlation of circumferential strains, the strain S-3 is identified to show the reverse phase to strains S-1, S-2 and S-4, and the tunnel, in the lateral direction, is considered to be governed by a shearing deformation as shown in Fig. 19. It is presumably due to a reason that the lateral deformation of the tunnel is governed by the propagation in the upward direction of shear waves in the surrounding rock.

6. CONCLUSION

According to the results obtained as above, the propagation of earthquake motion in deep rock at 260 m from the surface and accompanying deforming behavior of the cavern can be described as follows:

(1) In view of the fixed principal axes (principal axes II) along which the toal energy becomes the maximum, medium and minimum, the principal axes of earthquake motion in deep rock can be restricted in the horizontal plane for both maximum principal axis and intermediate principal axis. From the results of this observation, however, both of these two principal axes can be considered to have the possibility to

become relatively near the direction of epicenter, and it is rather difficult to difine the nearest of the two.

(2) In the case of principal axes (principal axes Ⅰ) varying in time domain (t) where the cross power spectrum at the time (t) becomes the maximum, medium and minimum, the vertical angle of the maximum principal axis is near 180° during the initial motion, and varies around 90° during and after the main motion, and it is assumed that the body wave is eminent in this observation site. Therefore, the primary wave (P wave) during the initial motion and the shear wave (S wave) during the main motion presumably propagate in the upward direction nearly vertically.

(3) The frequencies at the peaks of the amplification function are constant and not influenced by the properties of the earthquake. Also, in the horizontal plane of the rock around a tunnel, no noticeable amplification of the earthquake wave can be seen even in the vicinity of a cavern.

(4) Judging from the high correlation of any 2 points among the observation points, and from the phase of strains of the tunnel lining, the tunnel is governed by a first shearing deformation mode accompanying the propagation in the upward direction of the wave, the wavelength of which is very long.

7. POSTSCRIPT

The earthquake motion dealt in this text is small in scale and few in number, therefore, our understanding on the behavior based on the waveform analysis cannot be said to be the final yet. This observation will be continued further, and each time when a new earthquake motion is observed, the waveform analysis will be performed, and the descriptions given here will be reviewed ; it is considered necessary, by doing so, to further clarify our understanding on the earthquake behaviors.

ACKNOWLEDGEMENTS

As aforementioned, this observation was conducted in cooperation with JNR, and in this connection, we would like to express our sincere thanks to JNR's Tokyo Second Construction Bureau and those concerned to Railway Technical Research Institute for kindly permitting the publication of the observed results.

REFERENCES

1) Hayashi, M. and Komada, H. : Earthquake Records and Dynamic Analysis around the Underground Power House Cavern, Proceedings of the 6th Japan Earthquake Engineering Symposium, pp. 1873～1880, Dec., 1982.
2) Ichikawa, T. and Ariga, Y. : Seismic Behavior Observation of Underground Cavern, Proceedings of the 15th Japan National Conference on Earthquake Engineering, pp. 169～172, July, 1979.
3) Hamada, M. et al. : Observation and Study on Dynamic Behavior of Rock Cavern During Earthquake, Proceedings of the JSCE, No. 341, pp. 187～196, Jan., 1984.
4) Tamura, C. et al. : Maximum Acceleration of Earthquake in a Rock Site, Proceedings of the 15th Japan National Conference on Earthquake Engineering, pp. 181～184, July, 1979.
5) Charles H, Dowding. : Seismic Stability of Under-Ground Openings, The First International Symposium on Storage in excavated Rock Cavern Rock Store 77 Session 3, pp. 23～30, Sept., 1977.
6) Yoshikawa, K. : Earthquake Damage to Railway Tunnels in Japan, Advances in Tunnelling Technology and Sbsurface Use Vol. 4, No. 3, pp. 75～83, June, 1984.
7) Hoshiya, M. et al. : Principal Axes and Wave Characteristics of Ground Motion, Proceedings of the JSCE, No. 268, pp. 33～46, Dec., 1977.
8) Watabe, M. : Simulation of 3-Dimensional Earthquake Ground Motions, Annual Report of the Building Research Institute, pp. 201～206, 1974.
9) Nakamura, T., Asakura, T., Yamaguchi, Y, Tsujita, M. and Wakita, K. : Seismic Behavior of a Rock Tunnel —Analysis of Observed Wave—, Proceedings of the 6 th Japan Symposium on Rock Mechanics pp. 187～192, Dec., 1984.
10) Yamaguchi, Y., Tsujita, M., Wakita, K. and Arai, N. : Seismic Behavior of a Rock Tunnel —Principal Axes and Three Components of Observed Wave—, Proceedings of the 17 th Symposium on Rock Mechanics pp. 126～130, Feb., 1985.
11) Yamaguchi, Y., Tsujita, M., Wakita, K. and Arai, N. : The Characteristic of Three Components of Observed Earthquake Motion and Seismic Behavior of Rock Cavern, Proceedings of the 18th Japan National Conference on Earthquake Engineering, pp. 25～28, July, 1965.

(Received October 28 1985)